# Structure and Dynamics of Hydrated $NH_4^+$: An *ab initio* QM/MM Molecular Dynamics Simulation

PATHUMWADEE INTHARATHEP, ANAN TONGRAAR, KRITSANA SAGARIK
*School of Chemistry, Institute of Science, Suranaree University of Technology, Nakhon Ratchasima 30000, Thailand*

*Received 7 February 2005; Accepted 21 April 2005*
*DOI 10.1002/jcc.20265*
*Published online in Wiley InterScience (www.interscience.wiley.com).*

**Abstract:** A combined *ab initio* quantum mechanical/molecular mechanical (QM/MM) molecular dynamics simulation has been performed to investigate solvation structure and dynamics of $NH_4^+$ in water. The most interesting region, the sphere includes an ammonium ion and its first hydration shell, was treated at the Hartree–Fock level using DZV basis set, while the rest of the system was described by classical pair potentials. On the basis of detailed QM/MM simulation results, the solvation structure of $NH_4^+$ is rather flexible, in which many water molecules are cooperatively involved in the solvation shell of the ion. Of particular interest, the QM/MM results show fast translation and rotation of $NH_4^+$ in water. This phenomenon has resulted from multiple coordination, which drives the $NH_4^+$ to translate and rotate quite freely within its surrounding water molecules. In addition, a "structure-breaking" behavior of the $NH_4^+$ is well reflected by the detailed analysis on the water exchange process and the mean residence times of water molecules surrounding the ion.

 J Comput Chem 26: 1329–1338, 2005

**Key words:** $NH_4^+$; QM/MM; water exchange; mean residence time

## Introduction

Solvation structure and dynamics of ions in water play an important role in many chemical and biological systems.[1–4] Besides the simple alkaline and alkaline–earth metal cations, ammonium ion ($NH_4^+$) is an important chemical species that provides a simple model for solvated amides.[5,6] In addition, in compactly folded RNAs, coordination or hydrogen bonding of this ion in specific sites is a crucial aspect for its ability to stabilize the RNA fragment structure.[7] The detailed interpretation on the structure and dynamics of $NH_4^+$ in aqueous solution has been studied extensively.[8–20] Of particular interest, recent NMR measurements[6,8] have shown that $NH_4^+$ rotates quite fast in aqueous solution, despite the expected strong hydrogen bonding between the $NH_4^+$ and its surrounding water molecules. To explain such surprising phenomenon, several rotational mechanisms have been proposed based on either *ab initio* geometry optimizations[11–13] as well as Monte Carlo (MC)[14] and molecular dynamics (MD)[10,15–20] simulations. Most of the previous studies have provided useful information on the dynamical properties of the hydrated $NH_4^+$, such as its fast diffusive rotational motion. However, the agreement on the structure of the first solvation shell of $NH_4^+$, which is a necessary prerequisite for understanding its rotational mechanism, is still far from satisfactory. On the structural viewpoint of $NH_4^+$ in aqueous solution, the most representative picture of the coordination to emerge is of two groups of water molecules. There is a first group of four, which is strongly oriented so as to create nearly linear N—H···O interactions. This structural aspect is supported by experimental X-ray and neutron diffraction studies.[9,10] The second group of water molecules is much less strongly oriented than the first, and its structure is a source of major disagreement between the theoretical observations, consisting of 1–8 water molecules.[10,14–20] Thus, the comprehensive knowledge of how $NH_4^+$ interacts with water molecules remains incomplete.

Recently, MD simulation with polarizable models[17] has been performed to provide a qualitative prediction on the rotational dynamics of $NH_4^+$ in water, which is in good agreement with the experimental observations. However, the contributions of the ion's polarizability are not directly obtainable because there is no direct measurement of this quantity in aqueous solution, and the available data are usually extrapolations from ionic crystal and salt solu-

*Correspondence to:* A. Tongraar; email: anan_tongraar@yahoo.com

Contract/grant sponsor: The Thailand Research Fund under the Royal Golden Jubilee Ph.D. Program; contract/grant number: PHD/0225/2543 (to P.I. and K.S.)

Contact/grant sponsor: The Thailand Research Fund under the TRF Basic Research Grant (to A.T.)

**Table 1.** Average Binding Energies (in kcal mol$^{-1}$) and Average N—H···O Distances (in Å) of the Optimized $NH_4^+$-$(H_2O)_4$ Complex, Calculated at HF, DFT, and Higher Correlated Methods.

| Basis Set | DZV | | DZP | |
|---|---|---|---|---|
| Method | $E_{bond}$[a] (kcal mol$^{-1}$) | $R_{N-H\cdots O}$ (Å) | $E_{bond}$[a] (kcal mol$^{-1}$) | $R_{N-H\cdots O}$ (Å) |
| HF | −19.40 | 1.83 | −16.19 | 1.90 |
| BLYP | −21.61 | 1.74 | −18.26 | 1.78 |
| B3LYP | −21.89 | 1.74 | −18.44 | 1.78 |
| MP2 | −19.69 | 1.82 | −17.25 | 1.81 |
| MP4-DQ | −19.68 | 1.81 | −16.78 | 1.84 |
| CC-D | −19.70 | 1.82 | −16.73 | 1.84 |
| CI-D | −19.57 | 1.81 | −16.58 | 1.85 |

[a]The average values of energy per ligand.

tions.[21–24] Another attempt to obtain a reliable picture of $NH_4^+$ in water is based on first-principle simulation method introduced by Car and Parrinello (CP).[18] This approach relies on the density functional theory (DFT) at the BLYP level, and has been applied on a relatively small system of one $NH_4^+$ and 63 water molecules, which has been documented as a severe limitation of the CP-MD applicability for the treatment of electrolyte solutions.[25,26] In addition, although both exemplary approaches can provide quite reasonable detailed information on the rotational dynamics of $NH_4^+$ in water, the observed coordination numbers of 5.8[17] and 5.3[18] are considerably low when compared to the results from the X-ray measurement.[10]

Because both theoretical and experimental observations have provided a rather inhomogeneous picture of $NH_4^+$ in water, the motivation of the present work was to obtain more reliable data for the structure and dynamics of this hydrate complex. An alternative approach to elucidate such detailed information is to apply the so-called combined *ab initio* quantum mechanical/molecular mechanical (QM/MM) MD technique.[26–41] This technique has been proven to be a very reliable simulation scheme, which puts confidence in many new insights into composition, property, and reactivity of various solvated ions.[26–41] In the present study, therefore, the structural and dynamical properties of $NH_4^+$ in water will be investigated by means of *ab initio* QM/MM MD simulation.

## Methods

By the QM/MM technique,[26–30] the system is divided into two parts, namely the QM and MM regions. The total interaction energy of the system is defined as

$$E_{total} = \langle \Psi_{QM} | \hat{H} | \Psi_{QM} \rangle + E_{MM} + E_{QM-MM}, \quad (1)$$

where $\langle \Psi_{QM} | \hat{H} | \Psi_{QM} \rangle$ refers to the interactions within the QM region, while $E_{MM}$ and $E_{QM-MM}$ represent the interactions within the MM and between the QM and MM regions, respectively. The QM region is considered to be the chemically most important region, which includes $NH_4^+$ and its first hydration shell. It is treated by Born–Oppenheimer *ab initio* Hartree–Fock (HF) quantum mechanics, while the rest of the system is described by classical pair potentials. Basically, the reliability of the QM/MM results—besides the requirement of adequate simulation time—depends crucially on the QM size and the basis sets employed for describing all interactions within the QM region. According to the N—O radial distribution function (RDF) obtained by a preliminary pair potential simulation (data not shown), the first minimum of the N—O peak is located approximately at 3.8 Å. Within this region, about 8–12 water molecules are involved in the first solvation shell of $NH_4^+$. Thus, a QM diameter of 7.6 Å and a moderate basis set, like DZV,[42] seems to be acceptable within the available computational feasibility, leading to 4–8 min to compute quantum mechanical forces in each QM/MM MD step (on a DEC Alpha XP1000 workstation).

In principle, the inclusion of electron correlation in the quantum mechanical calculations can improve the quality of the simulation results, but this is far too time-consuming, even at the simple MP2 correlated level. To estimate the effects of electron correlation, geometry optimizations of the $NH_4^+$-$(H_2O)_4$ complex were conducted using *ab initio* calculations at different levels of theory. The average binding energies with basis set superposition error (BSSE) correction, and the average N—H···O distances calculated at HF, DFT, and highly correlated levels using DZV and DZP[42] basis sets are summarized in Table 1. The QM calculations with the DZP basis set were carried out to provide a systematic comparison of the effects of electron correlation, as well as to critically evaluate the adequacy of the DZV basis set employed in the present QM/MM MD simulation. In comparison to the results of the highly correlated methods, the neglect of electron correlation in the HF calculations yields slightly weaker binding energies with slightly larger N—H···O distances. In the opposite direction, the DFT calculations, either with BLYP or B3LYP functional, yield stronger binding energies and significantly short N—H···O distances, most probably caused by an overestimation of the correlation energy. This could be one of the reasons why the previous CP MD study,[18] using the BLYP functional, yielded a rather high rigidity of the ammonium hydrate complex. In general, the main advantage of the DFT, over the HF formalism, is that it uses the

**Table 2.** Optimized Parameters of the Analytical Pair Potential for the Interaction of Water with $NH_4^+$ (Interaction Energies in kcal $mol^{-1}$ and Distances in Å).

| Pair | $A$ (kcal $mol^{-1}$ Å$^5$) | $B$ (kcal $mol^{-1}$ Å$^7$) | $C$ (kcal $mol^{-1}$) | $D$ (Å$^{-1}$) |
|---|---|---|---|---|
| N—O | 305.575926 | 3783.8268 | −1794.3299 | 2.14078153 |
| N—H(W) | −3508.815861 | 1388.9633379 | 10361.9735 | 2.50568598 |
| H(A$^+$)—O | −349.7620287 | 176.0625425 | −9493.42614 | 3.79455210 |
| H(A$^+$)—H(W) | 27.04923252 | 23.91613451 | −31.5685243 | 1.039927027 |

exchange-correlation operator instead of the exchange operator, so it partially includes electron correlation according to the $E_{xc}[\rho]$ functional. However, because the extent of electron correlation included in DFT calculations is not exactly known, lower coordination numbers and the overly rigid structures were often found when using this method, especially for the treatment of ionic solutions.[26,35–38] From the data obtained in Table 1, it could be assumed, therefore, that the effects of electron correlation would have a minor influence on the ammonium–water interactions, and that the *ab initio* calculations at the HF level using DZV basis set are accurate enough to produce reliable structure and dynamics details of the hydrated $NH_4^+$. On the other hand, a comparison of the HF calculations with the DFT results with their inherent tendency towards lower coordination numbers and a too rigid hydration shell also appeared helpful to estimate the methodical boundaries.

During the QM/MM simulation, exchange of water molecules between the QM and MM region can occur frequently. In this case, the forces acting on each particle in the system are switched according to which region the water molecule is entering or leaving, and can be defined as

$$F_i = S_m(r)\,F_{QM} + (1 - S_m(r))\,F_{MM}, \tag{2}$$

where $F_{QM}$ and $F_{MM}$ are quantum mechanical and molecular mechanical forces, respectively. $S_m(r)$ is a smoothing function,[43]

$$\begin{aligned} S_m(r) &= 1, && \text{for } r \le r_1, \\ S_m(r) &= \frac{(r_0^2 - r^2)^2(r_0^2 + 2r^2 - 3r_1^2)}{(r_0^2 - r_1^2)^3}, && \text{for } r_1 < r \le r_0, \\ S_m(r) &= 0, && \text{for } r > r_0, \end{aligned} \tag{3}$$

where $r_1$ and $r_0$ are distances characterizing the start and the end of the QM region, applied within an interval of 0.2 Å (i.e., between the N—O distance of 3.8–4.0 Å) to ensure a continuous change of forces at the transition between the QM and MM regions.

For interactions within the MM and between the QM and MM regions, a flexible model,[44,45] which describes inter- and intramolecular interactions, was employed for water. The use of flexible model is favored over any of the popular rigid water models, to ensure compatibility and a smooth transition, when water molecules move from the QM region with their full flexibility to the MM region. The pair potential function for describing $NH_4^+$–$H_2O$ interactions was newly constructed using the Aug-cc-PVTZ basis set.[46–48] With respect to a symmetric tetrahedral geometry of the ammonium ion, 878 HF interaction energy points for various $NH_4^+$–$H_2O$ configurations, obtained from Gaussian98[49] calculations, were fitted to an analytical form of

$$\Delta E_{NH_4^+-H_2O} = \sum_{i=1}^{5}\sum_{j=1}^{3}\left[\frac{A_{ij}}{r_{ij}^5} + \frac{B_{ij}}{r_{ij}^7} + C_{ij}\exp(-D_{ij}r_{ij}) + \frac{q_i q_j}{r_{ij}}\right] \tag{4}$$

where $A$, $B$, $C$, and $D$ are the fitting parameters (see Table 2), $r_{ij}$ denotes the distances between the $i$-th atoms of ammonium ion and the $j$-th atoms of water molecule, and $q$ are atomic net charges. The Mulliken charges on N and H of $NH_4^+$, obtained from *ab initio* calculation using the Aug-cc-PVTZ basis set, and on O and H of the water molecule, which adopted from CF2 model,[44] were set to −0.5186, 0.3796, −0.6598, and 0.3299, respectively. It is known that, through ion–water interactions, these values change. However, the changes are partially compensated by the other terms in the potential during fitting to the *ab initio* energy surfaces.

The QM/MM MD simulation was performed in a canonical ensemble at 298 K. The temperature of the ensemble was kept constant using the Berendsen algorithm,[50] with a relaxation time of 0.1 ps. The cubic box, with a box length of 18.17 Å, contains one $NH_4^+$, and 199 water molecules with periodic boundary conditions. The Newtonian equations of motion were treated by a general predictor–corrector algorithm and the time step was set to 0.2 fs, which allowed for explicit movement of hydrogen atoms of $NH_4^+$ and water. The reaction-field method[51] was employed for the treatment of long-range interactions. The system was initially equilibrated by performing a QM/MM MD simulation, in which only the $NH_4^+$ was treated quantum mechanically, for 200,000 time steps. Then, the QM/MM simulation with a QM diameter of 7.6 Å, was started with the system's reequilibration for 30,000 time steps, followed by another 80,000 time steps to collect configurations every 10th step.

Because the characteristics of pure water represent a most important reference for the description of a hydrated ion, a comparison of the results with water data obtained at similar QM/MM level of accuracy was performed. Thus, the bulk properties discussed in this work refer to the properties of pure water obtained by a compatible simulation,[41] namely a QM/MM simulation with a QM diameter of 7.6 Å was carried out under the same conditions as reported in this work, simply replacing the ion by a water molecule.

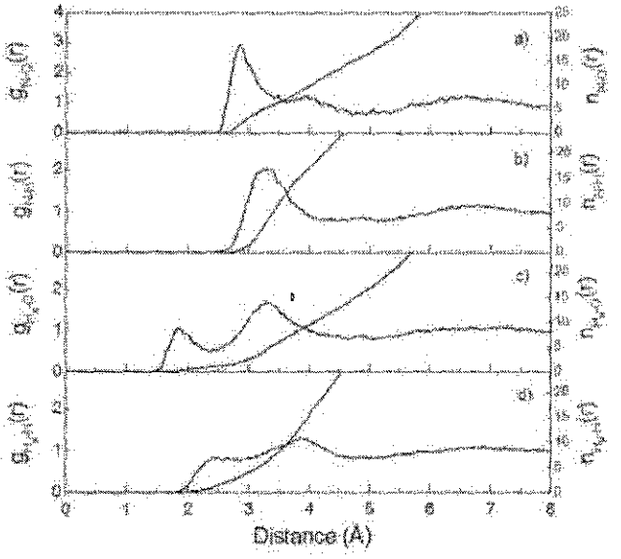


**Figure 1.** (a) N—O, (b) N—H, (c) $H_N$—O, and (d) $H_N$—H radial distribution functions and their corresponding integration numbers.

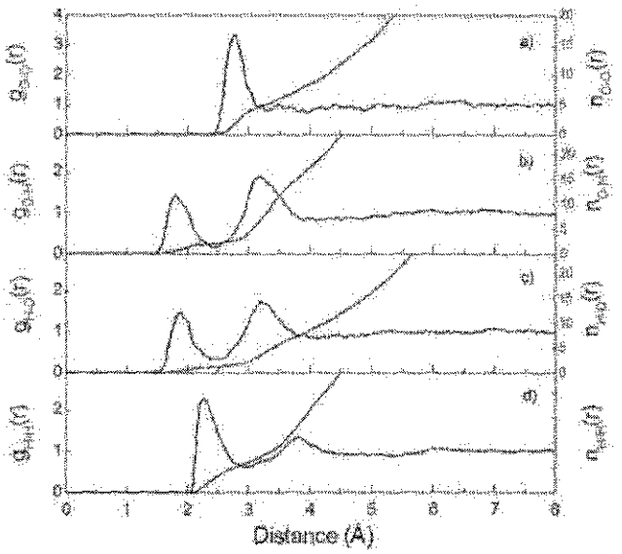


**Figure 2.** (a) O—O, (b) O—H, (c) H—O, and (d) H—H radial distribution functions and their corresponding integration numbers. The first atom of each pair refers to the atoms of the water molecule, whose oxygen position was defined as center of the QM region during the QM/MM simulation.

## Results and Discussion

### *Structural Properties*

The hydration structure of $NH_4^+$ is characterized by means of N—O, N—H, $H_N$—O, and $H_N$—H RDFs and their corresponding integration numbers, as shown in Figure 1. The QM/MM simulation reveals a broad unsymmetrical first N—O peak at 2.84 Å, together with considerable tailing up to around 4.7 Å. In comparison to the O—O RDF of bulk water, as depicted in Figure 2, the shape of N—O RDF indicates a high flexibility of the $NH_4^+$–water complex, as well as a high mobility of first-shell water molecules. In addition, the first minimum of the N—O peak is not well separated from the bulk, suggesting that water molecules surrounding the $NH_4^+$ are quite labile, and are loosely held by the ion. The observed hydration structure of $NH_4^+$ is significantly different to those obtained by the most recent MD simulations,[17,18] which reported rather well defined the first and even the second solvation shells of the ammonium ion. In the present QM/MM simulation, the minimum position of the N—O RDF may be roughly estimated to be 3.5 Å, where an integration up to this N—O range gives coordination number of 6.5 ± 0.2. Figure 3 shows the probability distributions of the number of surrounding water molecules, calculated within the N–O distances of 3.0, 3.5, and 4.0 Å, respectively. With respect to the N–O distance of 3.5 Å, a preferred coordination number of 6 is observed, followed by 7, 5, and 8 in smaller amounts. Apparently, numerous possible species of hydrated $NH_4^+$ exist, varying from 4- to 10-fold coordinated complexes. In fact, a small shift of N—O minimum will have significant impact on the coordination number. For example, at a slight larger N–O distance of 4.0 Å, the most frequent observed number of water molecules increases rapidly from 6 to 10. The QM/MM results demonstrate that numerous water molecules can mutually play a role in the hydrogen bond formation of $NH_4^+$ in water. Compared to the experimentally observed coordination number of 8,[10] good agreement can then be achieved. In fact, comparison between experiments and theories is not always straightforward because most of the experimental methods for structural analysis have to be performed with solutions of relatively high concentrations, while the theoretical approaches mostly refer to very dilute

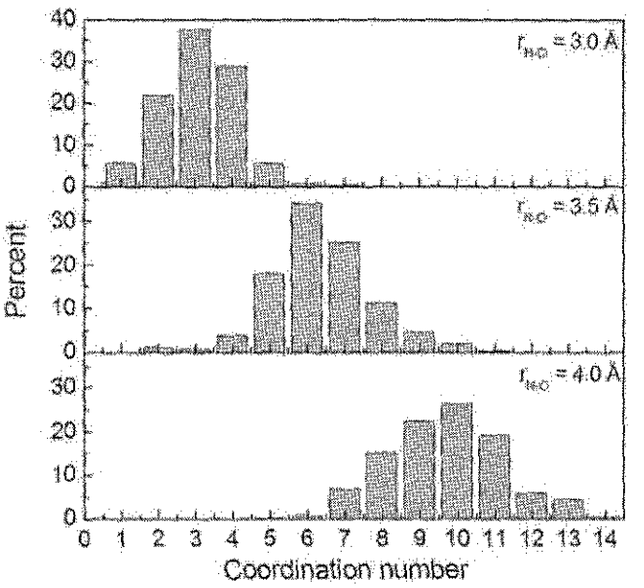


**Figure 3.** Coordination number distributions, calculated up to the N—O distances of 3.0, 3.5, and 4.0 Å, respectively.

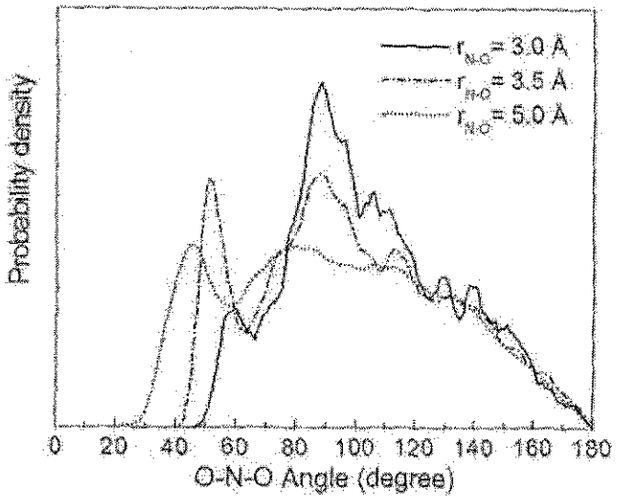


**Figure 4.** O–N–O angular distributions, calculated up to the N–O distances of 3.0, 3.5, and 5.0 Å, respectively.

solutions. As a consequence, a coordination number determined experimentally for high concentration solutions can be affected by coexisting counterions. Rapid ligand exchange poses another problem for the interpretation of experimental data, as it often leads to the simultaneous coexistence of several solvate species with different geometry and coordination number. When trying to fit a single (averaged) model to the spectroscopic data of such a system, errors will necessarily be introduced.

The hydrogen bonding between $NH_4^+$ and water can be interpreted via the $H_N$—O and $H_N$—H RDFs, as depicted in Figure 1c and d, respectively. The first $H_N$—O peak is centered at 1.84 Å, which is an indicative of hydrogen bonds between the ammonium hydrogens and their nearest-neighbor water molecules. Integrating up to the first $H_N$—O minimum yields about 1.1 waters, indicating that each of ammonium hydrogens coordinates to single water molecule. Compared to the O—H and H—O RDFs of pure water (Fig. 2b and c), the first $H_N$—O peak is not well separated from the second one, pointing at a more frequent and easy exchange of water molecules between the first shell and the outer region. Together with a rather broad N—H RDF, the QM/MM results clearly show that the hydrogen bonds between $NH_4^+$ and water is not extremely strong, in contrast to the recent MD simulations[17,18] which suggested that the first four water molecules formed a tight first solvation shell around the $NH_4^+$. From the QM/MM simulation, the hydration enthalpy of the $NH_4^+$ can be approximated by calculation of the energy difference between the ion–water and the water–water interactions of the solution and the water–water interaction energy of the pure water, under the identical conditions. In this work, the hydration enthalpy of $NH_4^+$ is estimated to be $-85.7$ kcal mol$^{-1}$, which is in good agreement with the experimental values of between $-84$ and $-89$ kcal mol$^{-1}$.[52-54]

Figure 4 displays the O–N–O angular distributions, calculated up to the N···O distances of 3.0, 3.5, and 5.0 Å, respectively. At short N···O distances, a tetrahedral cage structure of the hydrated $NH_4^+$ is recognizable by a pronounced large peak between 80–120°. The slight distortion from the ideally tetrahedral arrangement can be understood due to the interference between the first four water molecules that are directly hydrogen bonded to $NH_4^+$, with the other nearest-neighboring water molecules. It is obvious that some other nearest-neighbor water molecules can also position closely to the ion, even at a short N···O distance of 3.0 Å, as can be seen from a slight pronounced peak around 60°. This phenomenon is understandable because water molecules are quite small, in which many of them can form cluster around the ammonium ion. As a consequence, water molecules can involve in the hydrogen bond formation with the ion, and thus, providing the flexible structure of the $NH_4^+$–water complex.

Figure 5 illustrates the characteristics of the hydrogen bonds between $NH_4^+$ and water by means of the distributions of N—H···O angle, calculated within the $H_N$···O distances of 1.8, 2.0, and 2.5 Å, respectively. At the short $H_N$···O distances of 1.8 and 2.0 Å, the N—H···O hydrogen bonds are nearly linear, with peak maxima around 160–170°. Considering at the $H_N$···O distance of 2.5 Å, which corresponds to the first $H_N$—O RDF minimum, the probability of finding linear hydrogen bonds apparently decreases, while the pronounced peak between 90–140° becomes more significant. The latter peak implies the presence of multiple, nonlinear hydrogen bonds within the first solvation shell of each of ammonium hydrogens. The observed multiple coordination can be analyzed by plotting the H—N···O angular distributions, calculated within the N···O distance of 3.5 Å, as depicted in Figure 6. The two pronounced peaks around 0–30 and 90–120° correspond to the distributions of the four nearest-neighbor water molecules that form nearly linear hydrogen bonds to each of ammonium hydrogens. Apart from the water molecules that are directly hydrogen-bonded to the $NH_4^+$, it seems that other nearest-neighbor water molecules prefer to form bifurcated complex between two ammonium hydrogens. The preferred bifurcated structure of the nonhydrogen bonding waters, over the trifurcated one, can be recognizable from a more pronounced shoulder peak around 50–80°, compared to that of around 150–180°. The QM/MM results are in

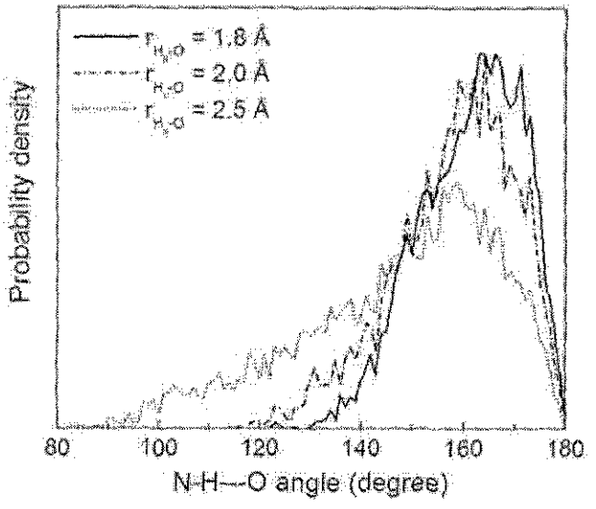


**Figure 5.** N—H···O angular distributions, calculated up to the $H_N$···O distances of 1.8, 2.0, and 2.5 Å, respectively.

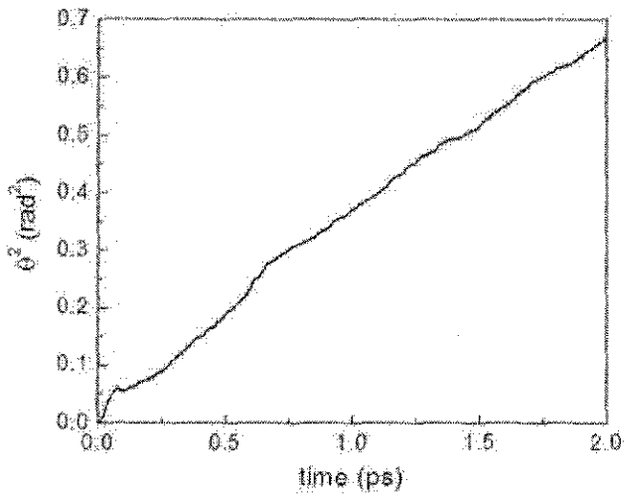


**Figure 10.** Mean-square angular displacements of $NH_4^+$ in water as a function of time.

where $\theta(t)$ denotes the angle formed by a vector in the body-fixed frame at with its initial direction ($\theta = 0$ at $t = 0$). The computed mean-square angle $\langle\theta(t)^2\rangle$ as a function of time is displayed in Figure 10, and the rotational diffusion constant estimated from the slope was $0.088 \times 10^{12}$ rad$^2$ s$^{-1}$, which is in good agreement with the experimental value of about $0.075 \times 10^{12}$ rad$^2$ s$^{-1}$ obtained by the NMR measurements.[6,8]

The ease of $NH_4^+$ rotation can be ascribed due to the presence of numerous water molecules around the ion that facilitate the rotation. Based on the QM/MM results, the most probable rotational dynamics of the $NH_4^+$ in water can be considered as follow. Because the hydrogen bond between $NH_4^+$ and water is not extremely strong, its strength maybe somewhat comparable to that of between water and water. Hence, when a number of water molecules interact with the ion, the first four nearest-neighbor waters are temporarily immobilized at each edge of the tetrahedral $NH_4^+$–water cage structure, while the others are more labile and are placed in bifurcated configurations between two ammonium hydrogens. Thus, it is obvious that because of the bifurcated waters that significantly enhance the ease for each of ammonium hydrogens to break its original hydrogen bond (with its original water molecule) and then to form a new hydrogen bond with another (bifurcated) water molecule. With sufficient amount of bifurcated waters, possibly up to six water molecules (according to the rough estimated first hydration shell, see Fig. 3), all possible reestablished N—H···O hydrogen bonds can easily occur along any rotational pathway of the $NH_4^+$. The QM/MM results support well a proposed multiple hydrogen bonding rotational mechanism,[8] and are in good agreement with the NMR experiments,[6] as well as being consistent with the reported rather low activation energy, $E_a$, for the reorientation of $NH_4^+$ in aqueous solution.[6,13,61]

*Water Exchange in the Hydration Shell of $NH_4^+$*

Within the total simulation time of 16 ps, several water exchange processes occurring at each of ammonium hydrogens are observed. To focus more distinctly on the water exchange processes, the plot of $H_N$···O distance is zoomed within the $H_N$···O distance of 4.0 Å and for only the first 8 ps of the QM/MM simulation trajectory, as depicted in Figure 11. It is obvious that water molecules surrounding the ammonium hydrogens can exchange by any of the proposed "classical" types, namely associative ($A$) and dissociative ($D$) as well as associative ($I_a$) and dissociative ($I_d$) interchange mechanisms.[62] These data confirm the structural lability of the $NH_4^+$ in aqueous solution, corresponding to the appearance of various possible species of the hydrate complex formed in the solution.

The rate of water exchange processes at each of ammonium hydrogens was evaluated by means of mean residence time (MRT) of the water molecules. In this work, the MRT values were calculated using a "direct" method,[63] being the product of the average number of nearest-neighbor water molecules located within the $H_N$···O distance of 2.5 Å with the duration of the QM/MM simulation, divided by the number of exchange events. Based on the direct accounting and setting various time parameter $t^*$, the MRT values are listed in Table 4. The time parameter $t^*$ has been defined as a minimum duration of the ligand's displacement from its original coordination shell. For such weakly hydrated $NH_4^+$, the $t^* = 0.5$ ps was proposed to be the best choice[63] as it corresponds to the mean lifetime of hydrogen bonds. With respect to this criterion, only the data obtained with $t^* = 0.0$ ps make sense for the estimation of H-bond lifetimes, while the MRT data obtained with $t^* = 0.5$ ps can be considered as a good measure for ligand exchange processes. In accordance with the $t^* = 0.5$ ps, an order of $\tau_{H_2O}(H_i) < \tau_{H_2O}$ ($H_2O$) is observed. The QM/MM results clearly show that water molecules binding to each of ammonium hydrogens are quite labile, and that the hydrogen bond between $NH_4^+$ and water is not very strong, allowing numerous water

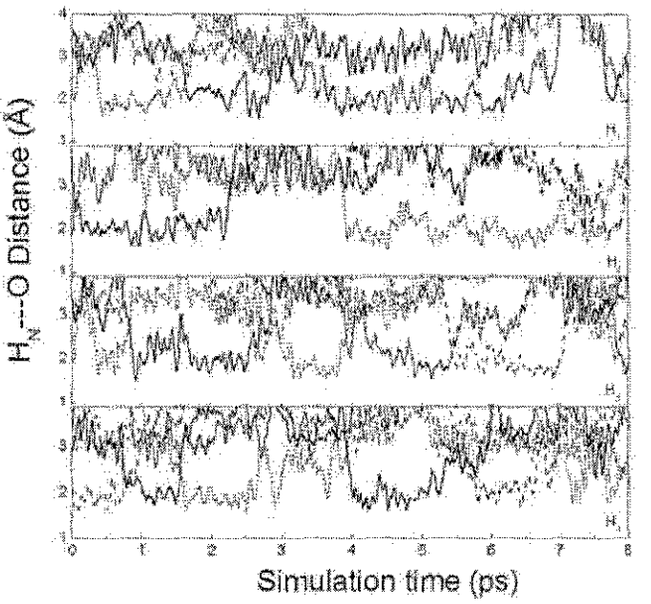


**Figure 11.** Water exchange in the first solvation shell of each of ammonium hydrogens, emphasizing for only the first 8 ps of the QM/MM simulation.

**Table 4.** Mean Residence Times of Water Molecules in Bulk and in the First Solvation Shell of Each of Ammonium Hydrogens, Calculated within the $H_N\cdots O$ Distance of 2.5 Å.

| | | | $t^* = 0$ ps | | $t^* = 0.5$ ps | |
|---|---|---|---|---|---|---|
| Solute/ion | CN | $t_{sim}$ | $N_{ex}^0$ | $\tau_{H_2O}^0$ | $N_{ex}^{0.5}$ | $\tau_{H_2O}^{0.5}$ |
| $H_1$ | 1.05 | 16.0 | 204 | 0.08 | 13 | 1.29 |
| $H_2$ | 1.14 | 16.0 | 231 | 0.08 | 12 | 1.52 |
| $H_3$ | 1.13 | 16.0 | 267 | 0.07 | 14 | 1.29 |
| $H_4$ | 1.08 | 16.0 | 227 | 0.07 | 13 | 1.33 |
| Pure $H_2O$[41] | 4.6 | 12.0 | 292 | 0.19 | 31 | 1.78 |

$N_{ex}$ is the number of accounted exchange events, $t_{sim}$ the simulation time in ps, and CN the average coordination number of the first hydration shell of water and of each of ammonium hydrogens.

exchange processes within the hydration sphere of the $NH_4^+$ to frequently occur. In addition, the MRT data also reveal the "structure-breaking" ability of the $NH_4^+$ in aqueous solution. The "structure-breaking" effect of the $NH_4^+$ can be recognized from its flexible hydration structure, as well as from the MRT values of water molecules surrounding the ion, which are smaller than that of the bulk. The QM/MM results suggest that the $NH_4^+$ cannot form a well-defined ion–water complex, and its influence can be concerned mainly to disrupt the solvent's hydrogen-bonded structure.

The detailed information on the solvation structure and dynamics of $NH_4^+$ in water is very crucial to fundamentally understand the reactivity of this ion in chemical and biological systems. For example, in the specific ion stabilization of the RNA structure, the potential of $NH_4^+$ to donate four hydrogen bonds in a tetrahedral geometry has been considered to responsible for its ability to stabilize the RNA fragment structure more effectively than the alkali metal cations.[7] Furthermore, because the RNA fragment selectivity for $NH_4^+$ is the result of a match between a tetrahedral array of hydrogen bond acceptors in the RNA and $NH_4^+$, the correct coordination or hydrogen bonding of $NH_4^+$ in specific sites is of particular importance to promote the correct conformation of the RNA.

## Conclusion

The combined *ab initio* QM/MM molecular dynamics simulation has provided more detailed descriptions on the structure and dynamics of $NH_4^+$ in water. The QM/MM simulation has revealed a flexible and more labile hydration structure of $NH_4^+$, in which numerous species of hydrated $NH_4^+$ appear, varying possibly from 4- to 10-fold coordinated complexes. Consequently, the observed fast translation and rotation of $NH_4^+$ in water can be understood due to its flexible hydration as well as the cooperative involvement of the multiple coordination that drives the ammonium ion to translate and rotate rather freely around its surrounding water molecules. In addition, the QM/MM simulation has demonstrated the behavior related to the "structure-breaking" ability of this ion in aqueous solution. We believe that the QM/MM results presented here are accurate, and that the QM/MM technique can be seen as a very promising tool to investigate the structural and dynamical properties of such highly labile $NH_4^+$ hydrate.

## References


1. Frank, H. S. Chemical Physics of Ionic Solutions; John Wiley & Sons: New York, 1956, p. 60.
2. Robinson, R. A.; Stokes, R. H. Electrolyte Solutions; Butterworth: London, 1959, 2nd ed.
3. William, R. J. P. Bio-inorganics Chemistry; Gould, R. F., Ed.; American Chemical Society: Washington, DC, 1971.
4. Hille, B. Ionic Channels of Excitable Membranes; Sinauer: Sunderland, MA, 1992, 2nd ed.
5. Perrin, C. L.; Gipe, R. K. J Am Chem Soc 1984, 96, 5631.
6. Perrin, C. L.; Gipe, R. K. J Am Chem Soc 1986, 108, 1088.
7. Wang, Y.; Lu, M.; Draper, D. E. Biochemistry 1993, 32, 12279.
8. Perrin, C. L.; Gipe, R. K. Science 1987, 238, 1393.
9. Hewish , N. A.; Neilson, G. W. Chem Phys Lett 1981, 84, 425.
10. Pálinkás, G.; Radnai, T.; Szász, G. I.; Heinzinger, K. J Chem Phys 1981, 74, 3522.
11. Jiang, J. C.; Chang, H.; Lee, Y. T.; Lin, S. H. J Phys Chem A 1999, 103, 3123.
12. Brugé, F.; Bernasconi, M.; Parrinello, M. J Chem Phys 1999, 110, 4734.
13. Kassab, E.; Evleth, E. M.; Hamou-Tahra, Z. D. J Am Chem Soc 1990, 112, 103.
14. Jorgensen, W. L.; Gao, J. J Phys Chem 1986, 90, 2174.
15. Karim, O. A.; Haymet, A. D. J. J Chem Phys 1990, 93, 5961.
16. Dang, L. X. Chem Phys Lett 1993, 213, 541.
17. Chang, T.; Dang, L. X. J Chem Phys 2003, 118, 8813.
18. Brugé, F.; Bernasconi, M.; Parrinello, M. J Am Chem Soc 1999, 121, 10883.
19. Szász, G. I.; Heinzinger, K. Z Naturforsch 1979, 34a, 840.
20. Bohm, H.; McDonald, I. R. Mol Phys 1984, 80, 887.
21. Jungwirth, P.; Tobias, D. J. J Phys Chem A 2002, 106, 379.
22. Tobias, D. J.; Jungwirth, P.; Parrinello, M. J Chem Phys 2001, 114, 7036.
23. Coker, H. J Phys Chem 1976, 80, 2078.
24. Pyper, N. C.; Pike, C. G.; Edwards, P. P. Mol Phys 1992, 76, 353.
25. Schwenk, C. F.; Loeffler, H. H.; Rode, B. M. Chem Phys 2001, 115, 10808.
26. Rode, B. M.; Schwenk, C. F.; Tongraar, A. J Mol Liq 2004, 110, 105.
27. Kerdcharoen, T.; Liedl, K. R.; Rode, B. M. Chem Phys 1996, 211, 313.
28. Tongraar, A.; Liedl, K. R.; Rode, B. M. J Phys Chem A 1997, 101, 6299.
29. Tongraar, A.; Liedl, K. R.; Rode, B. M. J Phys Chem A 1998, 102, 10340.
30. Marini, G. W.; Liedl, K. R.; Rode, B. M. J Phys Chem A 1999, 103, 11387.
31. Tongraar, A.; Rode, B. M. J Phys Chem A 2001, 105, 506.
32. Tongraar, A.; Sagarik, K.; Rode, B. M. J Phys Chem B 2001, 105, 10559.
33. Tongraar, A.; Sagarik, K.; Rode, B. M. Phys Chem Chem Phys 2002, 4, 628.
34. Tongraar, A.; Rode, B. M. Phys Chem Chem Phys 2003, 5, 357.
35. Schwenk, C. F.; Hofer, T. S.; Rode, B. M. J Phys Chem A 2004, 108, 1509.
36. Schwenk, C. F.; Rode, B. M. J Chem Phys 2003, 119, 9523.
37. Hofer, T. S.; Rode, B. M. J Chem Phys 2004, 121, 6406.
38. Schwenk, C. F.; Loeffler, H. H.; Rode, B. M. J Chem Phys 2001, 115, 10808.

39. Schwenk, C. F.; Loeffler, H. H.; Rode, B. M. J Am Chem Soc 2003, 125, 1618.
40. Tongraar, A.; Rode, B. M. Phys Chem Chem Phys 2004, 6, 411.
41. Tongraar, A.; Rode, B. M. Chem Phys Lett 2004, 385, 378.
42. Dunning, T. H., Jr.; Hay, P. J. Modern Theoretical Chemistry; Schaefer, H. F., Ed.; Plenum: New York, 1976.
43. Brooks, B. R; Bruccoleri, R. E.; Olafson, B. D.; States, D. J.; Swaminathan, S.; Karplus, M. J Comput Chem 1983, 4, 187.
44. Bopp, P.; Jancsó, G.; Heinzinger, K. Chem Phys Lett 1983, 98, 129.
45. Stillinger, F. H.; Rahman, A. J Chem Phys 1978, 68, 666.
46. Dunning, T. H., Jr. J Chem Phys 1989, 90, 1007.
47. Kendall, R. A.; Dunning, T. H., Jr.; Harrison, R. J. J Chem Phys 1992, 96, 6769.
48. Woon, D. E.; Dunning, T. H., Jr. J Chem Phys 1993, 98, 1358.
49. Frisch, M. J.; Trucks, G. W.; Schlegel, H. B.; Scuseria, G. E.; Robb, M. A.; Cheeseman, J. R.; Zakrewski, V. G.; Montgomery, J. A.; Stratmann, R. E.; Burant, J. C.; Dapprich, S.; Millam, J. M.; Daniels, A. D.; Kudin, K. N.; Strain, M. C.; Farkas, O.; Tomasi, J.; Barone, V.; Cossi, M.; Cammi, R.; Mennucci, B.; Pomelli, C.; Adamo, C.; Clifford, S.; Ochterski, J.; Peterson, G. A.; Ayala, P. Y.; Cui, Q.; Morokuma, K.; Malick, D. K.; Rabuck, A. D.; Raghavachari, K.; Foresman, J. B.; Cioslowski, J.; Ortiz, J. V.; Stefanov, B. B.; Liu, G.; Liashenko, A.; Piskorz, P.; Komaromi, I.; Gomperts, R.; Martin, R. L.; Fox, D. J.; Keith, T.; Al-Laham, M. A.; Peng, C. Y.; Nanayakkara, A.; Gonzalez, C.; Challacombe, M.; Gill, P. M. W.; Johnson, B. G.; Chen, W.; Wong, M. W.; Andres, J. L.; Head-Gordon, M.; Replogle, E. S.; Pople, J. A. GAUSSIAN 98; Gaussian, Inc.: Pittsburgh, PA, 1998.
50. Berendsen, H. J. C.; Postma, J. P. M.; van Gunsteren, W. F.; DiNola, A.; Haak, J. R. J Phys Chem 1984, 81, 3684.
51. Adams, D. J.; Adams, E. H.; Hills, G. J. Mol Phys 1979, 38, 387.
52. Arnett, E. M.; Jones, F. M.; Taagepera, M.; Henderson, W. G.; Beauchamp, J. L.; Holtz, D.; Taft, R. W. J Am Chem Soc 1972, 94, 4724.
53. Aue, D. H.; Webb, H. M.; Bowers, M. T. J Am Chem Soc 1976, 98, 318.
54. Klots, C. E. J Phys Chem 1981, 85, 3585.
55. McQuarrie, D. A. Statistical Mechanics; Harper & Row: New York, 1976.
56. Wishaw, B. F.; Stokes, R. H. J Am Chem Soc 1954, 76, 2065.
57. Gillen, K. T.; Douglass, D. C.; Hoch, M. J. R. J Chem Phys 1972, 57, 5117.
58. Woolf, L. A. J Chem Soc Faraday Trans 1 1975, 71, 784.
59. Sceats, M. G.; Rice, S. A. J Chem Phys 1980, 72, 3236.
60. Bopp, P. Chem Phys 1986, 106, 205.
61. Brown, R. J. C. J Mol Struct 1995, 345, 77.
62. Langford, C. H.; Gray, H. B. Ligand Substitution Processes; Benjamin, W. A. Inc. Press, New York, 1966.
63. Hofer, T. S.; Tran, H. T.; Schwenk, C. F.; Rode, B. M. J Comput Chem 2004, 25, 211.